Ferromagnetic ordering in Mn induced by thermal strain

Younghun Hwang, Jeongyong Choi, Soon Cheol Hong, and Sunglae Cho*
Department of Physics, University of Ulsan, Ulsan 680-749, Republic of Korea

Suk-Hee Han and Kyung-Ho Shin
Center for Spintronics Research, Korea Institute of Science and Technology, Seoul 136-791, Republic of Korea

Myung-Wha Jung
Department of Physics, Sogang University, Seoul 100-611, Republic of Korea
(Received 22 August 2008; published 16 January 2009)

We report that the thermal strain due to the thermal-expansion difference between a Mn film and a semiconductor substrate is strong enough to overcome the thermal energy for a paramagnetic (PM) state and also to break antiferromagnetic (AF) magnetic symmetry, inducing ferromagnetic (FM) ordering at high temperatures. A Mn film on GaAs (100) showed FM ordering up to 9000 Å with a Curie temperature (T_C) of over 750 K and a net magnetic moment of $0.33\mu_B$/Mn, instead of AF (Néel temperature, T_N=95 K) and PM orderings in bulk.

DOI: 10.1103/PhysRevB.79.045309 PACS number(s): 75.70.Ak, 73.43.Qt, 75.30.Kz

I. INTRODUCTION

An exchange integral (J_{ex}) determines the nature of the exchange interaction between magnetic ions, with a negative value indicating antiferromagnetic (AF) ordering and a positive value indicating ferromagnetic (FM) ordering. J_{ex} strongly depends on the distance between magnetic ions, as described in the Bethe-Slater curve.[1] In 3*d* transition metals, closely spaced magnetic ions prefer to be in an antiparallel spin alignment ($-J_{ex}$) in materials, such as Cr and Mn, and prefer to be in a parallel alignment ($+J_{ex}$) in materials such as Fe, Co, and Ni. It is theoretically predicted that while being nonmagnetic at compressed volumes, all transition metals become FM with high magnetic moments at sufficiently expanded volumes following Hund's rule and can ultimately be treated as free atoms.[2] As temperature increases, there is competition between exchange interaction and thermal energy, which eventually breaks magnetic ordering and induces paramagnetic (PM) behavior above T_C or T_N.

Bulk Mn is a particularly interesting material having five different crystal structures that change with temperature:[3,4] α-Mn is stable up to 727 °C, β-Mn between 727 and 1095 °C, γ-Mn between 1095 and 1133 °C, and δ-Mn between 1133 and 1244 °C (melting point). The α phase, which is stable at room temperature, has a body-centered-cubic (bcc) structure (bcc, a=8.911 Å, with 58 atoms per unit cell) and becomes a complex noncollinear AF below 95 K coupled to a tetragonal distortion in the crystal structure. The γ phase has a face-centered-cubic (fcc) structure (fcc, a=2.73 Å) and becomes AF below about 500 K.[5,6] The β-Mn (bcc, a=6.315 Å) and δ-Mn (bcc, a=3.0806 Å) phases are relatively unstable and show a spin glass of T_f =1.4 K and AF ordering, respectively.[3,4,7] It has been reported that as hydrostatic pressure increases, the T_N in the α phase shifts toward a lower temperature at a rate of 20 K/GPa up to 2 GPa (Ref. 8) and above 165 GPa; bcc α-Mn becomes a hexagonal close-packed (hcp) structure (ε phase, tentatively described), which is AFM.[9,10]

In epitaxial thin films on crystalline substrates, various crystallographic and magnetic phases other than those seen in bulk material have been predicted. These are made possible by additional driving forces such as broken bonding at the surface, interface interaction, and lattice mismatch strain between the substrate and film, etc. Strain is known to be a powerful tool in modifying the structural, electronic, and magnetic properties of a material because the energies associated with structural and magnetic changes have a similar order of magnitude (~0.1 eV/atom).[11] It has been reported that AF materials, such as Cr and Mn, showed surface ferromagnetism in several monolayer thin films.[12–14]

Here we report that thermal strain due to the difference in the coefficient of thermal expansion between a Mn film and its semiconductor substrate is not negligible and is strong enough to overcome the thermal energy for a paramagnetic state and also to break AF magnetic symmetry to induce ferromagnetic ordering. We observed that a stable α-Mn film on GaAs (100) showed FM ordering up to 9000 Å with a T_C of above 750 K rather than AF and PM orderings. It showed a net magnetic moment of $0.33\mu_B$/Mn, which might be an important characteristic in the technological spintronic device community because typical AF materials used in spin devices are Mn-based alloys, such as FeMn, NiMn, IrMn, PtMn, and RhMn, with relatively high thermal-expansion coefficients.

II. EXPERIMENT

We have grown Mn thin films on GaAs (100) substrate at the following temperatures: 30, 100, 200, 300, 400, and 500 °C. For the growth of Mn epilayers, we used a molecular-beam epitaxy (MBE) system, VG Semicon model V80; it consists of growth, analysis, and load-lock chambers and is equipped with reflection high-energy electron diffraction (RHEED). The base pressure of the growth chamber was in the 10^{-10} Torr range. After thermal annealing in an As flux to remove surface oxide at 600 °C for 30 min, we deposited a 3000 Å GaAs buffer layer on the GaAs (100) substrate at 500 °C. Standard effusion cells were used for Mn

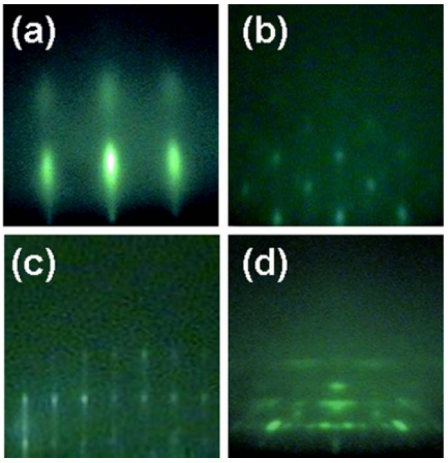

FIG. 1. (Color online) RHEED patterns of 200 Å Mn thin films grown on GaAs(100) substrate along the $[1\bar{1}0]$ azimuth at different substrate temperature: (a) 30, (b) 300, (c) 400, and (d) 500 °C.

and Ga evaporations, while cracking effusion cell was used for As evaporation (Veeco Co.). The growth of Mn epilayers was 0.5 Å/s. The rate of evaporation was confirmed by quartz-crystal microbalance and ion gauge beam flux monitor. The crystal structure of the grown film was investigated using x-ray diffraction [(XRD) model D/max-RC, Rigaku Co., Tokyo, Japan] studies. For the magnetization measurements, we used a magnetic property measurement system [(MPMS) Quantum Design, Inc.] in the temperature range of 5–400 K and vibrating sample magnetometer [(VSM) Lake Shore Cryotronics, Inc. 7300] in the temperature range of 300 and 750 K.

III. RESULTS AND DISCUSSION

Figure 1 shows the series of the RHEED patterns of Mn films grown at 30–500 °C along the $[1\bar{1}0]$ GaAs substrate direction. The RHEED patterns for bcc α-Mn thin film grown at 200–500 °C were spotty, indicating the rough surfaces in good agreement with the surface topography by atomic and magnetic force microscopy (AFM and MFM) measurements.

Figure 2(a) shows the room-temperature θ-2θ XRD patterns of the 1000 Å Mn films. We have observed that the samples grown at 30 and 100 °C have a fcc γ phase with (001) growth direction, while the samples grown at above 200 °C have the bcc α phase with (110) growth direction. Figure 2(b) shows both the lattice constants perpendicular to the film ($a_\perp$) and the strains of the α-Mn films as functions of growth temperatures. The lattice constants were smaller than the known bulk value of 8.911 Å and decreased with increasing growth temperature up to 400 °C, indicating tensile strain in films which became stronger with increased growth temperature. The strain perpendicular to the plane of the Mn film ($\varepsilon_\perp$) as a function of growth temperature was calculated using $\varepsilon_\perp=(a-a_\perp)/a$, where a and $a_\perp$ are the bulk and thin-film Mn lattice constants, as shown in Fig. 2(b). For the sample grown at 400 °C, the measured $a_\perp$ is 8.812 Å at room temperature, generating a strain of 1.1×10^{-2}.

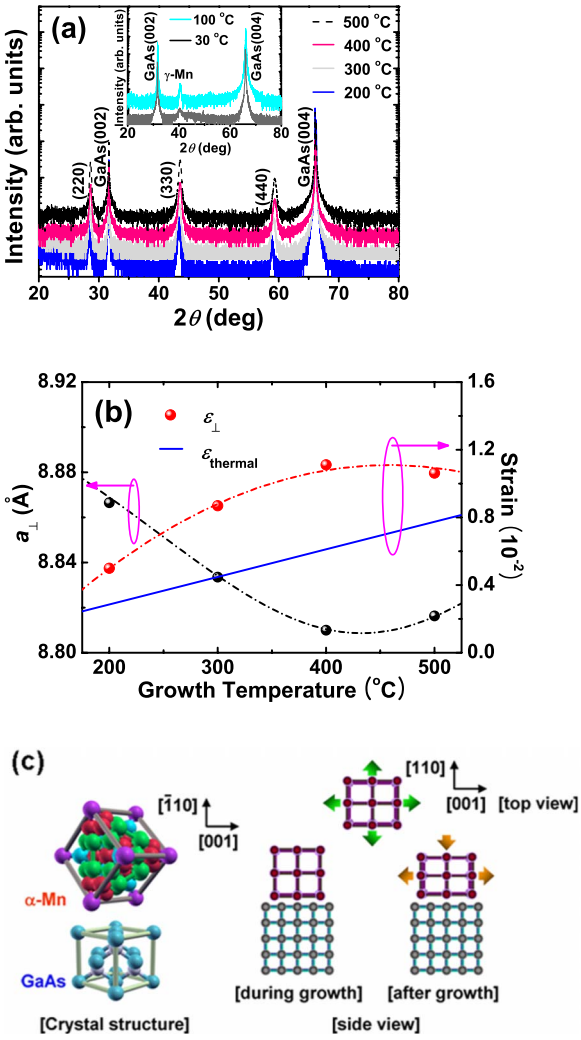

FIG. 2. (Color online) Structural properties of Mn films on GaAs(001). (a) θ-2θ XRD patterns of Mn films grown at 30, 100, 200, 300, 400, and 500 °C. The samples grown at 30 and 100 °C show the fcc γ phase with (001) growth direction, while the samples grown at above 200 °C show the bcc α phase with (110) growth direction. (b) The lattice parameters ($a_\perp$) perpendicular to the film (black circles) and the estimated strain (red circles and blue line) of the Mn film as functions of growth temperature. The strain ($\varepsilon_\perp$) perpendicular to the plane was calculated using the $\varepsilon_\perp=(a-a_\perp)/a$, where a is the bulk Mn lattice. The thermal strain can be described by the equation, $\varepsilon_{thermal}=K(\alpha_{Mn}-\alpha_{GaAs})\Delta T$, where K describes the value of the lattice relaxation, and α_{Mn} and α_{GaAs} are the thermal-expansion coefficients of Mn and GaAs, respectively. (c) A simple illustration of the tensile strain occurrence in bcc α-Mn due to the thermal-expansion coefficients. Mn film on substrate grows in a volume dependant upon growth temperature. When the sample cools down to room temperature after growth, both the film and the substrate are compressed. The film is compressed because of the higher Mn thermal expansion, which induces the tensile strain.

Considering only the strain due to lattice mismatch, these observations are opposite than we expected because the lattice constant of bulk bcc α-Mn (110) is larger than that of GaAs (a=5.654 Å). The lattice mismatches between bulk bcc α-Mn (110) and GaAs (a=5.654 Å) are 4.8% or 10.25%, in the (100) and (110) directions, respectively, re-

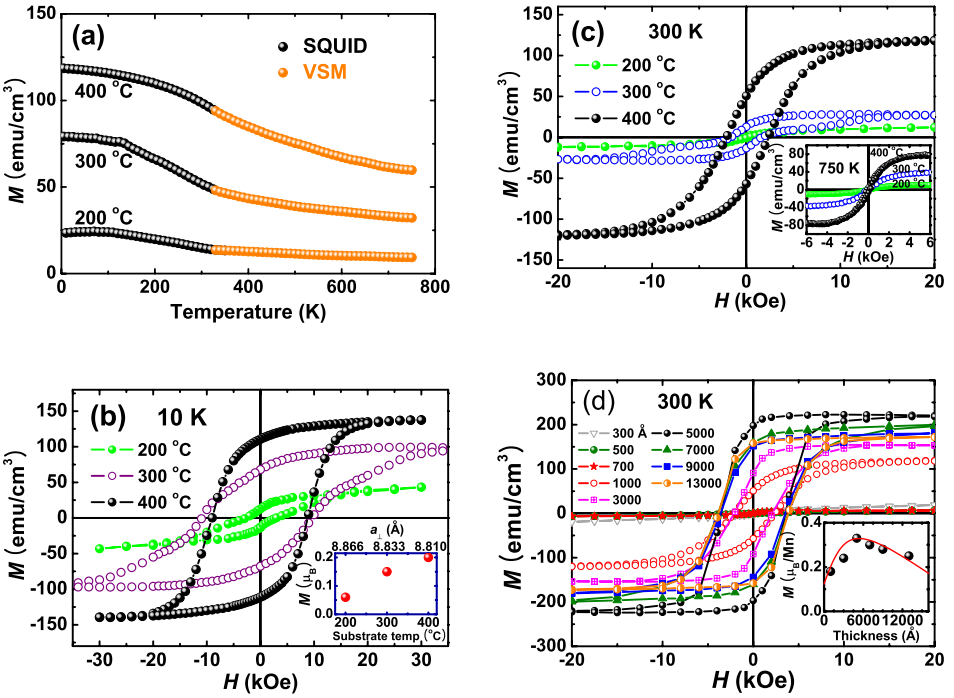

FIG. 3. (Color online) Magnetic properties of Mn films. (a) Temperature-dependent magnetization (M) of Mn films grown at 200, 300, and 400 °C in a magnetic field of 3 kOe. (b) Magnetic hysteresis loops with magnetic field perpendicular to the film at 10 K. The inset of (b) shows the net magnetic moments at 10 K as a function of growth temperature determined from the saturated magnetization. (c) Magnetic hysteresis loops with magnetic field perpendicular to the film at 300 K. The inset of (c) shows the hysteresis loops at 750 K. (d) Thickness-dependent hysteresis loops at 300 K. The highest magnetic moment per Mn is $0.33\mu_B$ in 5000 Å, as shown in the inset.

sulting in compressive strain. The estimated critical thicknesses, following the simple Beam formula[15] for strain relaxation in a Mn film on GaAs, were 93 and 43 Å. Hence, the compressive strain due to the lattice mismatch was almost relaxed in the 1000 Å film thickness. The observed tensile strain may be due to the difference in thermal-expansion coefficients between the α-Mn ($\alpha_{\mathrm{Mn}}=21.7\times10^{-6}$ K^{-1} at 300 K) and the GaAs ($\alpha_{\mathrm{GaAs}}=5.4\times10^{-6}$ K^{-1} at 300 K).[16] The thermal strain ($\varepsilon_{\mathrm{thermal}}$) can be described by the equation, $\varepsilon_{\mathrm{thermal}}=K(\alpha_{\mathrm{Mn}}-\alpha_{\mathrm{GaAs}})\Delta T$, where K describes the value of the lattice relaxation and ΔT is the temperature difference between the growth and the measured temperatures. For films that are thick enough, K might be set to 1 because the strain due to the lattice mismatch could be assumed to be fully relaxed. The thermal strain at room temperature for the sample grown at 400 °C is estimated to be approximately 6.1×10^{-3}, using the room-temperature constants α_{Mn} and α_{GaAs}. As growth temperature increases, the thermal strain increases, resulting in a decrease in lattice constant with growth temperature. Figure 2(c) illustrates that the Mn thin films on GaAs are tensely strained due to the thermal-expansion coefficients. The Mn film grows in a volume dependant upon the growth temperature. During growth, the lattice mismatch strain is relaxed in about 100 Å and when the sample cools down to room temperature after growth, both the film and the substrate are shrunk. Thus, the film is compressed because of the higher Mn thermal-expansion coefficient, which induces a tensile strain. Note that the magnetostrictive strains induced by the magnetization of a ferromagnet in a magnetic field via domain-wall rotation and migration of the transition metals Fe, Co, and Ni are very small, in the order of 10^{-5} for Fe. Also note that negative thermal expansion was reported below 95 K in bulk Mn, indicating the correlation between antiferromagnetism and thermal expansion below 95 K.

Figures 3(a)–3(c) show the temperature-dependent magnetizations (M) and magnetic hysteric loops with the perpendicular magnetic field of Mn films of 1000 Å grown at 200, 300, and 400 °C. Interestingly, the samples show well-defined magnetic hysteresis, indicating that the α-Mn films grown at 200, 300, and 400 °C are ferromagnetic with a Curie temperature (T_C) above 750 K. M and the coercive field increase with increasing growth temperature. The average magnetic moments of the Mn films determined from the saturated magnetization increased remarkably from $0.06\mu_B$ in the 200 °C film to $0.20\mu_B$ in the 400 °C film, as shown in the inset of Fig. 3(b). Thickness-dependent hysteric loops with the perpendicular magnetic field are shown in Fig. 3(d). The magnetic moments at 300 K ranged between 120 and 220 emu/cm^3, resulting in the highest magnetic moment for Mn of $0.33\mu_B$ in 5000 Å thick Mn film grown at 400 °C, as shown in the inset of Fig. 3(d). From the magnetization loop, the nonrectangular hysteric behavior was observed in a magnetic field parallel to the film (not shown here), while the rectangular behavior was observed in the perpendicular field as mentioned, indicating the presence of magnetic anisotropy. The 300, 500, and 700 Å thick samples did not show well-defined hysteresis, which might be due to the competition between lattice mismatch-induced compressive forces and thermal strain-induced tensile forces. Thus, we may conclude that the increased strain and magnetization with growth temperature, as well as the ferromagnetic ordering in α-Mn thin films on GaAs (100) up to temperatures of 750 K, can be attributed to the thermal strain between the Mn film and GaAs substrate. Note that for the samples grown at 30 and 100 °C, AF ordering was observed in the Mn film at room temperature, which is consistent with the previous results for fcc γ-phase Mn.

Figures 4(a)–4(f) are atomic force microscopy topographic images and MFM images of 1000, 9000, and 1 3000 Å thick Mn films grown at 400 °C. The Mn film surface topography is rough, which was confirmed by the

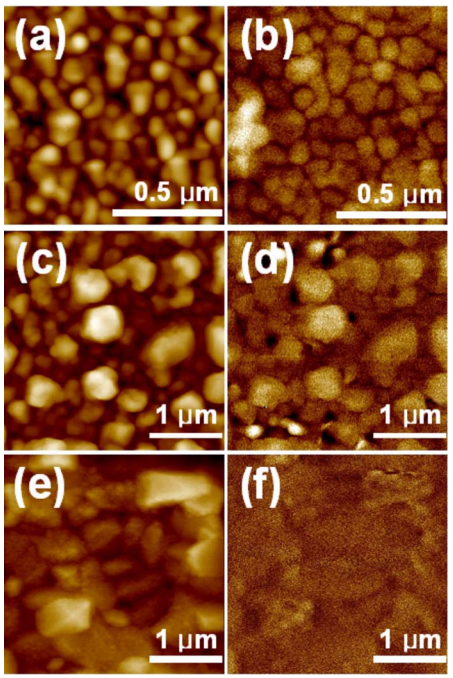

FIG. 4. (Color online) Topography and magnetic structure of Mn films. (a) Atomic force microscopy image of 1000 Å thick Mn film. (b) MFM image of 1000 Å film. (c) Atomic force microscopy image of 9000 Å film. (d) MFM image of 9000 Å film. (e) Atomic force microscopy image of 13 000 Å film. (f) MFM image of 13 000 Å film.

spotty RHEED patterns. Up to 9000 Å, surprisingly, we were able to observe the magnetic domain in the surface of the Mn films, as shown in Fig. 4(d). The magnetic domain image disappeared in the 1 3000 Å thick film. These results indicate that the Mn samples have domain formation up to 9000 Å, which is consistent with the results of the magnetization features on the Mn film. After 9000 Å, the thermal strain relaxed.

In order to investigate the correlations between magnetization and carrier transport on these films, electrical resistivity, magnetoresistance (MR), and the Hall-effect measurements were performed. The samples grown at high temperatures showed higher electrical resistivity at room temperature and showed a slope change around 95 K, as shown in Fig. 5(a), corresponding to the T_N in bulk α-Mn and 600 K. Figures 5(b) and 5(c) show the MR versus magnetic field curves for the 400 °C grown Mn film at different measuring temperatures. Note that the applied magnetic field is perpendicular to the film. At temperatures above 95 K, a decrease in MR with magnetic field, i.e., negative MR, and a strong hysteresis were observed, as shown in Fig. 5(b). The negative MR is due to the decreased scattering centers caused by the increase in magnetic domain with the increased magnetic field, which is also evidence of FM ordering in the Mn film. At temperatures below 95 K, a monotonous increase in resistance with increasing magnetic field is observed for all MR curves [Fig. 5(c)], which is probably due to the dominant ordinary magnetoresistance (OMR) effect.[17] The OMR is the increase in resistance with increased magnetic field due to bending of the electron trajectories by the Lorentz force. Figure 5(d) shows the magnetic-field dependence of the Hall resistance at various temperatures for 400 °C grown Mn film. The Hall resistance R_{Hall} is given by the sum of the ordinary Hall-effect (OHE) due to the Lorentz force and the anomalous Hall effect (AHE), originating from the asymmetric scattering in the presence of magnetization. Clear hysteresis and remanence at all temperatures are observed consistent with FM hysteric data.

PM to FM transition is observed in intermetallic compounds made of FM and non-FM elements such as Fe_3Al,[18] FeAl,[19] CoAl,[20] CoGa,[21] Ni_3Sn_2,[22] Fe_3Ge_2,[22] Pt_3Fe,[23] and

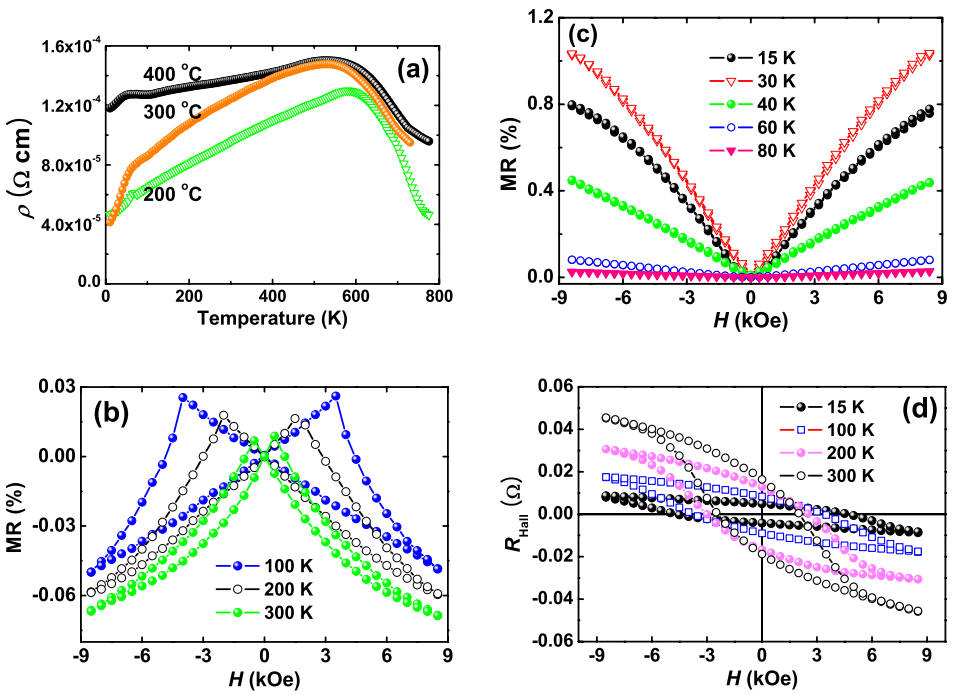

FIG. 5. (Color online) Magnetotransport properties for α-Mn thin film. (a) Temperature dependence of the zero-field electrical resistivities. (b) MRs of 400 °C grown film at 15, 30, 40, 60, and 80 K. (c) MRs of 400 °C grown film at 100, 200, and 300 K in a perpendicular magnetic field. (d) Anomalous Hall resistance R_{Hall} of 400 °C grown Mn film at 15, 100, 200, and 300 K. Clear hysteresis are observed.

Fe_2AlMn,[24] when they are severely ball milled or crushed so that FM atoms gather together to interact with each other. The α-Mn phase is known to have a noncollinear magnetic structure with four different magnetic moments $2.83\mu_B$, $1.82\mu_B$, $0.43\mu_B$, and $0.45\mu_B$ from four inequivalent lattice sites.[25] For this reason, α-Mn is sometimes considered to be an intermetallic compound because of the four different magnetic and electronic configurations in each unit cell. Thus, the thermal strains along (110) in the Mn thin film modify the distances between Mn atoms, which might result in FM ordering over 750 K. Electronic calculation is needed for better understanding.

IV. CONCLUSION

The thermal strain due to the difference in the thermal-expansion coefficients of a α-Mn film and GaAs substrate has enough energy to overcome the thermal energy for a paramagnetic state and also to break AF magnetic symmetry to induce ferromagnetic ordering. We expect similar phenomena in other Mn-based AF alloys such as FeMn, NiMn, IrMn, PtMn, and RhMn. We also predict that epitaxial Mn clusters on a GaAs matrix in a GaMnAs diluted magnetic semiconductor or GaAs/Mn digital alloys, typically grown at 250 °C, might show FM ordering above room temperature with the same reason.

ACKNOWLEDGMENTS

This work was supported by the Korea Science and Engineering Foundation (KOSEF) through the National Research Laboratory program funded by the Ministry of Science and Technology (Grant No. R0A-2006-000-10241-0) and the SRC/ERC program (Grant No. R11-2000-071) and the KIST vision 21 program.

*slcho@ulsan.ac.kr

[1] B. D. Cullity, *Introduction to Magnetic Materials* (Addison-Wesley, Reading, MA, 1972).
[2] V. L. Moruzzi and P. M. Marcus, Phys. Rev. B **38**, 1613 (1988).
[3] D. Hobbs, J. Hafner, and D. Spišák, Phys. Rev. B **68**, 014407 (2003).
[4] J. Hafner and D. Hobbs, Phys. Rev. B **68**, 014408 (2003).
[5] J. E. Zimmerman, A. Arrott, H. Sato, and S. Shinozaki, J. Appl. Phys. **35**, 942 (1964).
[6] H. Yamagata and K. Asayama, J. Phys. Soc. Jpn. **33**, 400 (1972).
[7] H. Nakamura, K. Yoshimoto, M. Shiga, M. Nishi, and K. Kakurai, J. Phys.: Condens. Matter **9**, 4701 (1997).
[8] A. Miyake, T. Kanemasa, R. Yagi, T. Kagayama, K. Shimizu, Y. Haga, and Y. Ōnuki, J. Magn. Magn. Mater. **310**, e222 (2007).
[9] H. Fujihisa and K. Takemura, Phys. Rev. B **52**, 13257 (1995).
[10] M. Eder, J. Hafner, and E. G. Moroni, Phys. Rev. B **61**, 11492 (2000).
[11] L. M. Falicov, D. T. Pierce, S. D. Bader, R. Gronsky, K. B. Hathaway, H. J. Hopster, D. N. Schuller, and R. H. Victora, J. Mater. Res. **5**, 1299 (1990).
[12] W. Drube and F. J. Himpsel, Phys. Rev. B **35**, 4131 (1987).
[13] W. L. O'Brien and B. P. Tonner, Phys. Rev. B **51**, 617 (1995).
[14] M. Albrecht, M. Maret, J. Köhler, B. Gilles, R. Poinsot, J. L. Hazemann, J. M. Tonnerre, C. Teodorescu, and E. Bucher, Phys. Rev. Lett. **85**, 5344 (2000).
[15] J. Singh, *Semiconductor optoelectronics-Physics and Technology* (McGraw-Hill, New York, 1995).
[16] D. R. Lide, *CRC Handbook of Chemistry and Physics*, 84th ed. (CRC, Boca Raton, FL, 2003).
[17] J. P. Jan, Solid State Phys. **5**, 1 (1957).
[18] M. J. Besnus, A. Herr, and A. J. P. Meyer, J. Phys. F: Met. Phys. **5**, 2138 (1975).
[19] Y. Yang, I. Baker, and P. Martin, Philos. Mag. B **79**, 449 (1999).
[20] L. M. Di, H. Bakker, Y. Tamminga, and F. R. deBoer, Phys. Rev. B **44**, 2444 (1991).
[21] L. M. Di, H. Bakker, and F. R. de Boer, Physica B **182**, 91 (1992).
[22] G. F. Zhou and H. Bakker, Phys. Rev. B **49**, 12507 (1994).
[23] S. Takahashi and K. Ikeda, J. Phys. Soc. Jpn. **52**, 2772 (1983).
[24] I. Baker, D. Wu, M. Wittmann, and P. R. Munroe, Mater. Charact. **52**, 209 (2004).
[25] A. C. Lawson, Allen C. Larson, M. C. Aronson, S. Johnson, Z. Fisk, P. C. Canfield, J. D. Thompson, and R. B. Von Dreele, J. Appl. Phys. **76**, 7049 (1994).